ESAIM: PROCEEDINGS AND SURVEYS, **March 2015, Vol. 50, p. 133-143**
Franck BOYER, Thierry GALLOUET, Raphaèle HERBIN and Florence HUBERT Editors

A WELL-BALANCED SCHEME FOR A TRANSPORT EQUATION WITH VARYING VELOCITY AND IRREGULAR OPACITIES

Thomas Leroy[1]

Abstract. An equation for photons containing a frequency drift term modeling the Doppler effects and an emission absorption coefficient is considered. On the one hand, this frequency drift term involves a coefficient κ relative to the fluid velocity with which the photons interact. This coefficient may vanish, leading to numerical difficulties. On the second hand, the emission absorption σ is known to be very irregular with respect to the frequency, and thus the design of well-balanced scheme is a mathematical issue. In this work are presented new numerical results for the spectrally well-balanced scheme in the context of highly irregular opacities.

1. Introduction

The aim of this work is to extend the recent study [7] to highly irregular emission absorption coefficients. The coupling between the transport equation for photons and an equation describing the evolution of a moving fluid involves several parameters. In particular, the emission absorption coefficient σ is known to be very irregular with respect to the frequency. It yields mathematical difficulties, in particular to prove theoretical results as existence of solutions (see for example [2,3]). This kind of equations is complicated to solve, and thus reduced models are an interesting issue. Recently (see [8]), the non-equilibrium regime has been studied in the context of a relativistic gas of photons interacting with a moving fluid, and the convergence in this regime of the solution of the relativistic transfer equation to the solution of a diffusion equation involving a frequency drift term has been proved. The corresponding homogeneous (in space) equation is

$$\begin{cases} \partial_t \rho = \dfrac{\kappa}{3}\nu\partial_\nu\rho + \sigma(\nu)(B(\nu)-\rho) & \text{in } [0,T]\times\mathbb{R}^+_\nu, \\ \rho(0,\nu) = \rho^{in}(\nu), \end{cases} \tag{1.1}$$

where $\rho = \rho(t,\nu)$ is the density of photons at time t and at frequency ν, $B(\nu) = \nu^3\left(e^\nu - 1\right)^{-1}$ is the Planck function, σ is the emission absorption coefficient, $\kappa \in [-\kappa^*, \kappa^*], \kappa^* > 0$ is the divergence of the fluid velocity and T is a given final time such that $0 < T < +\infty$. The design of costless numerical schemes for this equation is an interesting issue. Since radiative phenomena are very fast compared to hydrodynamic ones, well-balanced schemes are a possible solution. As mention in [7], classical "Greenberg-Leroux" type well-balanced schemes [4] (see also [6] for a recent review on the topic) constructed by discretizing the source terms at the interfaces and by using a Godunov scheme on the obtained equation are not consistent with equation (1.1) in the regime $\kappa \to 0$. This explains the introduction of the spectrally well-balanced scheme (SWB), for which a uniform (with respect to the wave velocity κ) convergence result has been provided. On the

[1] CEA, DAM, DIF, F-91297 Arpajon, France, and Laboratoire Jacques-Louis Lions, Université Pierre et Marie Curie, 75252 Paris Cedex 05, France, thomas.leroy@ljll.math.upmc.fr

other hand and as mentioned before, the emission absorption coefficient is highly irregular, and plays an important role from the physical point of view. It is thus necessary to report faithfully this behavior. In a first approach a very fine mesh could be used, but it is not possible in general in photons' transport. Indeed the distribution function of the photons is often rather peaked in frequency. In this context and due to the frequency shift, the classical upwind scheme is not accurate enough.

In this paper the behavior of the spectrally well-balanced scheme is studied for several irregular opacities, and its numerical solution is compared with the Greenberg Leroux and upwind schemes. In particular numerical tests are performed with a coefficient σ constructed as the sum of a regular part and peaked functions, which seems to be realistic, and with the so called Cramer's opacity. The well-balanced property and the consistency as $\kappa \to 0^{\pm}$ of the spectrally well-balanced scheme are shown to be preserved for such opacities.

This paper is organized as follows. In a first part the different schemes of interest and their properties are recalled. In particular the behavior of each schemes as $\kappa \to 0^{\pm}$ and their dependence (via the CFL) with respect to the emission absorption coefficient σ are pointed out. In a second part numerical results for different configurations of the parameters κ and σ, involving in particular irregular opacities, are presented. The consistency of the SWB scheme as $\kappa \to 0^{\pm}$ even for irregular σ is shown numerically. Finally, the interest of the SWB scheme in comparison to the upwind scheme will be illustrated with test cases in which the relative L^1 error of the upwind scheme can reach 35%.

2. A review of well-balanced schemes

Let us consider a frequency domain $\mathbb{D} = [\varepsilon, \hat{\nu}]$, for given $0 < \varepsilon < \hat{\nu} < +\infty$ and, for $1 \leq j \leq N$, an irregular mesh defined by $(N+1)$ points $\varepsilon = \nu_{\frac{1}{2}} < ... < \nu_{N+\frac{1}{2}} = \nu^*$. The middle of the j-th frequency band is denoted as ν_j, i.e. $\nu_j = (\nu_{j-\frac{1}{2}} + \nu_{j+\frac{1}{2}})/2$ and its length is denoted as $\Delta\nu_j$. We also define the dual $(j+\frac{1}{2})$-th frequency band as the cell $[\nu_j, \nu_{j+1}]$, which length is denoted $\Delta\nu_{j+\frac{1}{2}}$. We denote $h = \max_j \Delta\nu_j$ and we assume that there exists a constant C such that $\forall j \in \{1, ..N\}\,,\ 0 < Ch \leq \Delta\nu_j$.

The parameter ε is introduced only for technical reasons, since the opacities σ discussed in the next sections may have a singularity as $\nu \to 0$ (Cramer's opacity, part 3.2). Since the aim of this paper is the design of well-balanced schemes, it is necessary to study the stationary equation associated to (1.1)

$$\begin{cases} \dfrac{\kappa}{3}\nu\partial_\nu\rho + \sigma(\nu)(B(\nu) - \rho) = 0 \qquad \text{in } [0, \hat{\nu}], \\ \rho(\nu^*) = \rho^*, \end{cases} \tag{2.1}$$

where $\nu^* = \hat{\nu}$ if $\kappa > 0$, which yields a transport of the photons toward the frequency $\nu = 0$, and $\nu^* = 0$ if $\kappa < 0$, which yields a transport of the photons toward the frequency $\nu = \hat{\nu}$. Obviously this equation can be solved and one has

$$\rho\big(\nu; \rho^*, \nu^*\big) = \rho^* e^{-\frac{3}{\kappa}\int_\nu^{\nu^*} \frac{\sigma(s)}{s} ds} + \frac{3}{\kappa}\int_\nu^{\nu^*} \frac{\sigma(s)B(s)}{s} e^{-\frac{3}{\kappa}\int_\nu^s \frac{\sigma(\tau)}{\tau} d\tau} ds. \tag{2.2}$$

This solution has a limit as $\kappa \to 0^{\pm}$:

$$\lim_{\kappa \to 0^{\pm}} \rho\big(\nu; \rho^*, \nu^*\big) = B(\nu). \tag{2.3}$$

This stationary solution will be used in the next parts to construct well-balanced schemes.

2.1. " Classical " well-balanced scheme

In this part a first well-balanced scheme for equation (1.1) is introduced. Its construction uses the method developed by J.M. Greenberg and A.Y. Leroux [4]: discretizing the source term at the interfaces, one uses a Godunov scheme on the obtained equation. It yields the following scheme, denoted as the WB1 scheme

$$\begin{cases} \dfrac{d}{dt}\rho_j = \dfrac{\kappa}{3}\nu_j \dfrac{\rho(\nu_j;\rho_{j+1};\nu_{j+1}) - \rho_j}{\Delta\nu_j}, & 1 \le j \le N-1, \quad \kappa > 0, \\ \dfrac{d}{dt}\rho_j = \dfrac{\kappa}{3}\nu_j \dfrac{\rho_j - \rho(\nu_j;\rho_{j-1};\nu_{j-1})}{\Delta\nu_j}, & 2 \le j \le N, \quad \kappa < 0, \end{cases} \tag{2.4}$$

with the natural boundary conditions $\rho_N(t) = \rho(t,\nu_N)$ in the case $\kappa > 0$ and $\rho_1(t) = \rho(t,\nu_1)$ in the case $\kappa < 0$, where $\rho(t,\nu)$, defined in (3.1) is the analytical solution of equation (1.1). Considering a classical explicit Euler discretization of the time derivative, the CFL is given by

$$\Delta t \le \max_j \frac{3\Delta\nu_j}{|\kappa|\nu_j}. \tag{2.5}$$

It is interesting to note that the CFL of this scheme does not depend on σ, but depends on the wave velocity κ. A simple Taylor expansion of the exponential functions in the stationary solution shows the consistency of this scheme for any fixed and non zero κ. On the other hand, this scheme is not consistent as $\kappa \to 0^{\pm}$. Indeed, the limit of the stationary solution in this regime (2.3) yields

$$\lim_{\kappa\to 0^{\pm}} \frac{d}{dt}\rho_j = 0, \tag{2.6}$$

which obviously is not a consistent discretization of equation (1.1) as $\kappa = 0$. This explain the introduction of a new class of well-balanced schemes.

2.2. Spectrally Well-Balanced scheme

In this part is recalled the Spectrally Well-Balanced scheme [7], whose construction uses the integrating factor $M(\nu^*;\nu) = e^{-\frac{3}{\kappa}\int_{\nu}^{\nu^*}\sigma(s)s^{-1}ds}$. It is defined by

$$\begin{cases} \dfrac{d}{dt}\rho_j = \dfrac{\sigma(\nu_j)}{1 - M(\nu_{j+1};\nu_j)}\Big(\rho\big(\nu_j;\rho_{j+1},\nu_{j+1}\big) - \rho_j\Big), & 1 \le j \le N-1, \quad \kappa > 0, \\ \dfrac{d}{dt}\rho_j = \dfrac{\sigma(\nu_j)}{1 - M(\nu_{j-1};\nu_j)}\Big(\rho\big(\nu_j;\rho_{j-1},\nu_{j-1}\big) - \rho_j\Big), & 2 \le j \le N, \quad \kappa < 0, \end{cases} \tag{2.7}$$

where the boundary conditions are the same than for the WB1 scheme (2.4). Considering once again a classical explicit Euler discretization of the time derivative, the CFL is given by

$$\begin{cases} \Delta t \le \max_j \dfrac{1 - M(\nu_{j+1};\nu_j)}{\sigma(\nu_j)}, & \kappa > 0, \\ \Delta t \le \max_j \dfrac{1 - M(\nu_{j-1};\nu_j)}{\sigma(\nu_j)}, & \kappa < 0. \end{cases} \tag{2.8}$$

On the contrary to the previous scheme, the CFL of the SWB scheme strongly depends on the L^{∞} norm of the opacity σ. Indeed, one has

$$\lim_{\sigma\to\infty} \Delta t = 0.$$

On the other hand, it is interesting to see that it is the integrating factor that allows to recover a consistent limit scheme as $\kappa \to 0^{\pm}$. Indeed, the limit (2.3) as $\kappa \to 0^{\pm}$ of the stationary solution

together with the relation $\lim_{\kappa\to 0^\pm} M(\nu_{j\pm1};\nu_j)=0$ lead to

$$\lim_{\kappa\to 0^\pm}\frac{d}{dt}\rho_j=\sigma(\nu_j)\big(B(\nu_j)-\rho_j\big). \tag{2.9}$$

The semi-discrete SWB scheme (2.7) has been proved to be uniformly (with respect to the parameter κ) convergent, result which is recalled here and whose proof can be founded in [7].

Lemma 2.1 (Uniform convergence)**.** *We define $\rho_h=(\rho_j)_{1\le j\le N}$ and the discrete norm $\|\,.\,\|_{L^2_d}$ such that $\|\rho_h\|^2_{L^2_d}=\sum_j \Delta\nu_{j+\frac12}\rho_j^2$. Assume that the initial data satisfies $\rho^{in}\in H^2(\mathbb{D})$. Assume moreover that the emission absorption coefficient satisfies $\sigma\in W^{2,\infty}(\mathbb{D})$ and that there exists a constant $\sigma_*>0$ such that $\forall\nu\in\mathbb{D},\sigma(\nu)\ge\sigma_*$. Then the numerical solution of the semi-discrete scheme (2.7) satisfies the following estimate, where the constant $C(T)$ is uniform in $\kappa\in(0,\kappa^*]$: $\|\rho_{ex}(t)-\rho_h(t)\|_{L^2_d}\le C(T)h$, $0<t<T$.*

The assumption on the regularity of the opacity σ has no particular physical meaning, but for technical reasons is necessary to obtain the convergence in L^2.

2.3. **Upwind scheme**

In all the forthcoming numerical results, the numerical solutions of the well-balanced schemes (2.4) and (2.7) are compared to the following classical upwind scheme

$$\begin{cases}\dfrac{d}{dt}\rho_j=\dfrac{\kappa}{3}\dfrac{\rho_{j+1}-\rho_j}{\Delta\nu_j}\nu_{j+\frac12}+\sigma(\nu_j)\big(B(\nu_j)-\rho_j\big), & 1\le j\le N-1, \quad \kappa>0,\\[2ex] \dfrac{d}{dt}\rho_j=\dfrac{\kappa}{3}\dfrac{\rho_j-\rho_{j-1}}{\Delta\nu_j}\nu_{j-\frac12}+\sigma(\nu_j)\big(B(\nu_j)-\rho_j\big), & 2\le j\le N, \quad \kappa<0,\end{cases} \tag{2.10}$$

where once again the boundary conditions are the same than for the WB1 scheme (2.4). Considering once again a classical explicit Euler discretization of the time derivative, the CFL is given by

$$\begin{cases}\Delta t\le 3\ \max\limits_j\ \dfrac{\Delta\nu_j}{\kappa\nu_{j+\frac12}+3\Delta\nu_j\sigma(\nu_j)}, & \kappa>0,\\[2ex] \Delta t\le 3\ \max\limits_j\ \dfrac{\Delta\nu_j}{-\kappa\nu_{j-\frac12}+3\Delta\nu_j\sigma(\nu_j)}, & \kappa<0.\end{cases} \tag{2.11}$$

As for the previous SWB scheme, the CFL of the upwind scheme strongly depends on the L^∞ norm of σ. Obviously the upwind scheme is consistent in both regimes $\Delta\nu_j\to 0$ and $\kappa\to 0^\pm$.

3. Numerical results

In this section numerical results are presented for the " classical " well-balanced scheme WB1 (2.4), the Spectrally well-balanced scheme SWB (2.7) and the upwind scheme (2.10) in several configurations of the coefficients κ and σ. This section is divided in two parts. In a first part the long time behavior and the consistency as $\kappa\to 0^\pm$ of the schemes of interest are studied for highly irregular emission absorption coefficients σ. The main point is that the SWB scheme exactly capture the numerical solution as time goes on and is consistent as $\kappa\to 0^\pm$. In a second part we study several configurations of the parameters κ and σ in which the relative L^1 error of the upwind scheme is maximized.

Since this study involves a very simple model, the analytical solution of equation (1.1) can be computed, and its expression is given by

$$\rho(t,\nu)=\rho^{in}(\nu e^{\frac{\kappa}{3}t})e^{-\frac{3}{\kappa}\int_\nu^{\nu e^{\frac{\kappa}{3}t}}\sigma(\tau)\tau^{-1}d\tau}+\int_0^t\sigma\big(\nu e^{\frac{\kappa}{3}s}\big)B\big(\nu e^{\frac{\kappa}{3}s}\big)e^{-\frac{3}{\kappa}\int_\nu^{\nu e^{\frac{\kappa}{3}s}}\sigma(\tau)\tau^{-1}d\tau}ds, \tag{3.1}$$

Since one of the regime of interest is $|\kappa| << 1$, it is numerically necessary to use a non singular form of this analytical solution. To this end one remarks that the expression under the integral can be integrated by parts. One finds

$$\begin{aligned}\rho(t,\nu) = B(\nu) + \Big(\rho^{in}(\nu e^{\frac{\kappa}{3}t}) - B\big(\nu e^{\frac{\kappa}{3}t}\big)\Big) e^{-\frac{3}{\kappa}\int_\nu^{\nu e^{\frac{\kappa}{3}t}} \sigma(\tau)\tau^{-1}d\tau} \\ + \frac{\kappa}{3}\nu \int_0^t e^{\frac{\kappa}{3}s} B'\big(\nu e^{\frac{\kappa}{3}s}\big) e^{-\frac{3}{\kappa}\int_\nu^{\nu e^{\frac{\kappa}{3}s}} \sigma(\tau)\tau^{-1}d\tau} ds,\end{aligned} \tag{3.2}$$

which is no longer singular in κ. The same procedure is applied to treat the singularity in the stationary solution (2.2). The following relative L^1 error is introduced, where the final time T^f will be defined for each test case

$$\frac{\|\rho_j(t) - \rho(\nu_j, t)\|}{\|\rho(\nu_j, T^f)\|}. \tag{3.3}$$

For all the numerical tests a random mesh composed of 50 cells is considered. The domain is $\mathbb{D} = [\varepsilon, 30]$, where ε varies between 0 and 10^{-1} according to the different opacities. The initial conditions are taken as $\rho^{in}(\nu) = B(\nu - 15)$ if $\kappa > 0$ and $\rho^{in}(\nu) = 0$ if $\kappa < 0$ and the boundary conditions are given by the analytical solution (3.2).

3.1. **Highly irregular σ**

Many physical contexts implies highly irregular emission absorption coefficient σ, whose frequency dependence is sometimes regular and sometimes very peaked. The numerical study of such opacities is thus interesting. Numerically, the coefficient σ is constructed as the sum of a regular part and peaked functions (cf figure 1)

$$\sigma(\nu) = \frac{150}{1+\nu} + \sum_{1\le j\le 20} P_j, \tag{3.4}$$

where the peaked functions are distributed regularly on the mesh. In this part ε is taken equal to 0, so the domain is $[0, 30]$.

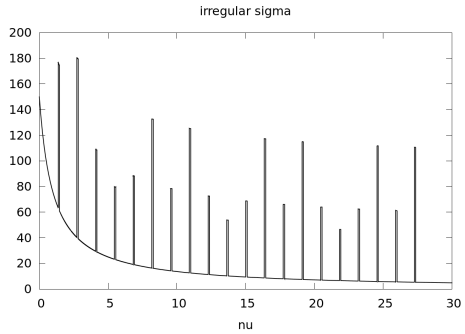

FIGURE 1: Irregular emission absorption coefficient

The choice of σ (3.4) yields an exact numerical integration of all the integrals in the analytical solution (3.2). In the same way, the integrals in the expression of the stationary solutions (2.2) are numerically computed exactly. The first property to verify numerically is the well-balanced property of the SWB (and WB1) scheme. In figure 2 are displayed the time evolution of the relative L^1 error of the SWB, WB1 and upwind scheme for $\kappa = 1$ and $\kappa = -1$. As expected, both the SWB and the WB1 schemes exactly capture the stationary solution, but it is interesting to notice that the WB1 scheme is much slower than the SWB scheme.

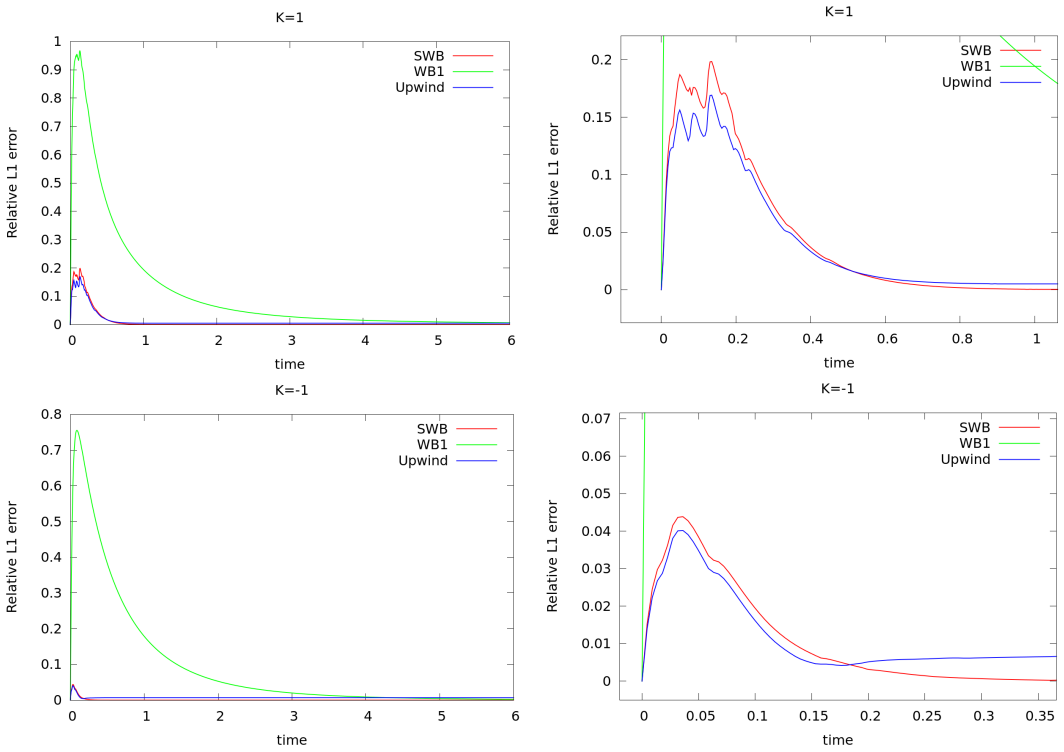

FIGURE 2: L^1 Relative error vs time, $T^f = 6$. Top: $\kappa = 1$, bottom: $\kappa = -1$

As explain in the previous section, the SWB scheme is uniformly (in κ) convergent, and this property has to be checked numerically for this choice of σ. Figure 3 displays the evolution, as $\kappa \to 0^{\pm}$, of the L^1 error between the solutions of the SWB, WB1 and the upwind schemes and the numerical solution of the following scheme, consistent with equation (1.1) as $\kappa = 0$:

$$\frac{d}{dt}\rho_j = \sigma(\nu_j)\big(B(\nu_j) - \rho_j\big). \tag{3.5}$$

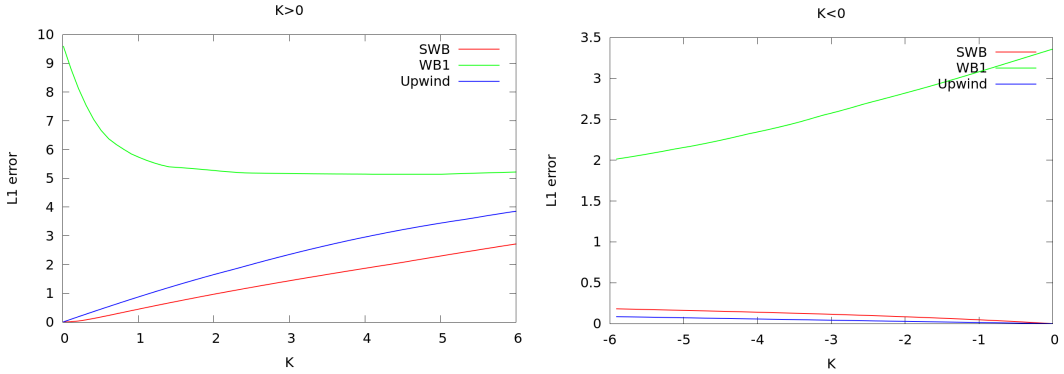

FIGURE 3: L^1 error vs κ. Left: $\kappa > 0$, t=0.1. Right: $\kappa < 0$, t=0.02

Figure 4 displays, in a (Log,Log) scale, the L^1 error of the schemes with respect to the number of cells. It shows that as expected, all the schemes are of order 1.

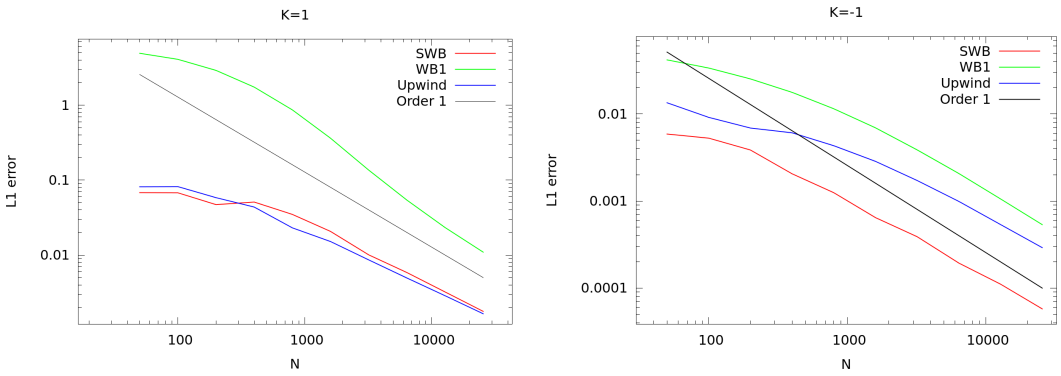

FIGURE 4: L^1 error vs N, (Log,Log) scale. Left: $\kappa > 0$, t=0.1. Right: $\kappa < 0$, t=0.02

3.2. **Cramer's opacity**

In this part we study the behavior of the schemes with the Cramer's opacity:

$$\sigma(\nu) = \frac{1 - e^{-\nu}}{\nu^3}. \tag{3.6}$$

This opacity leads to $\sigma(\nu)B(\nu) = e^{-\nu}$, and has a singularity as $\nu \to 0$. For this coefficient the analytical value of the integrals in the expression of solutions (1.1) and (2.1) can no longer be computed analytically. Numerically, they are computed by classical five points Gaussian quadratures. In this part and due to the singularity of the opacity, ε is taken equal to 10^{-1} and thus the domain is $[10^{-1}; 30]$. The same study than for the previous opacity is performed, and as before the long time behavior of the numerical solutions of the schemes is studied. In figure 5 are displayed the time evolution of the relative L^1 error of the schemes. Once again and as expected, the SWB and WB1 schemes exactly capture the stationary solution, while the relative error of the upwind scheme is 18% for $\kappa = 1$ and 7% for $\kappa = -1$.

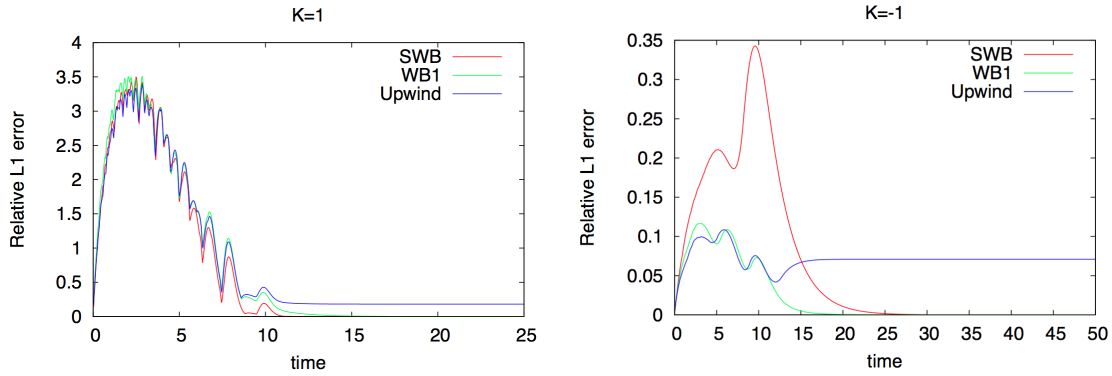

FIGURE 5: Relative L^1 error vs time. Left: $\kappa = 1$, $T^f = 25$, right: $\kappa = -1$, $T^f = 50$

As before, the behavior of the schemes for $\kappa \to 0^{\pm}$ is studied. Figure 6 displays the error between the schemes and the numerical solution of the scheme (3.5) as $\kappa \to 0^{\pm}$. It shows that the SWB scheme is consistent with equation (1.1), even for small coefficient κ.

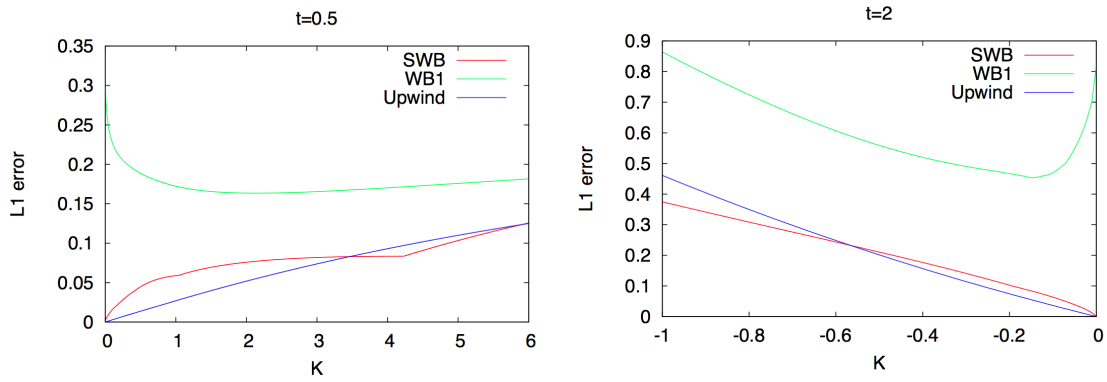

FIGURE 6: L^1 error vs κ. Left: $\kappa > 0$, t=0.5. Right: $\kappa < 0$, t=2

3.3. **SWB vs upwind**

In this part the advantage of the SWB scheme compared with the upwind scheme is highlighted. Indeed, for certain values of κ and σ, the upwind L^1 error can become significant. In the previous part, for σ defined in (3.4) and $\kappa = \pm 1$, the upwind relative L^1 error was of order 1%. On the other hand we have seen that for the Cramer's opacity and for $\kappa = 1$, the relative L^1 error of the upwind scheme reaches 18%, which is non negligible. Two test cases are presented here in which the upwind relative L^1 error is significant. In both the case we take σ as a piecewise constant function. In the first following one, the discontinuity is placed at the middle of the mesh (figure 7).

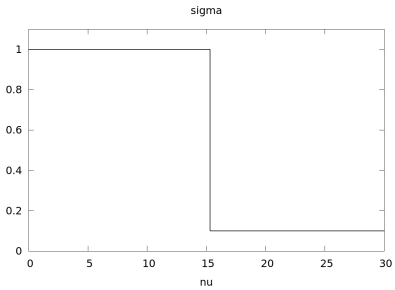

FIGURE 7: Piecewise constant emission absorption coefficient

Figure 8 displays the relative L^1 error of the schemes as the time increases for several value of κ. The initialization is such that $\rho^{in}(\nu) = B(\nu - 15)$. It shows that while increasing the coefficient κ, the relative L^1 error of the upwind scheme also increases, and reach roughly 35% in the case $\kappa = 10$.

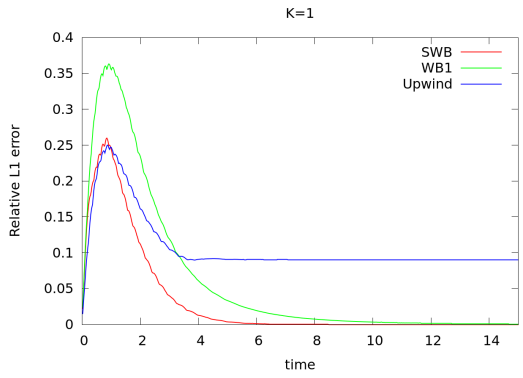

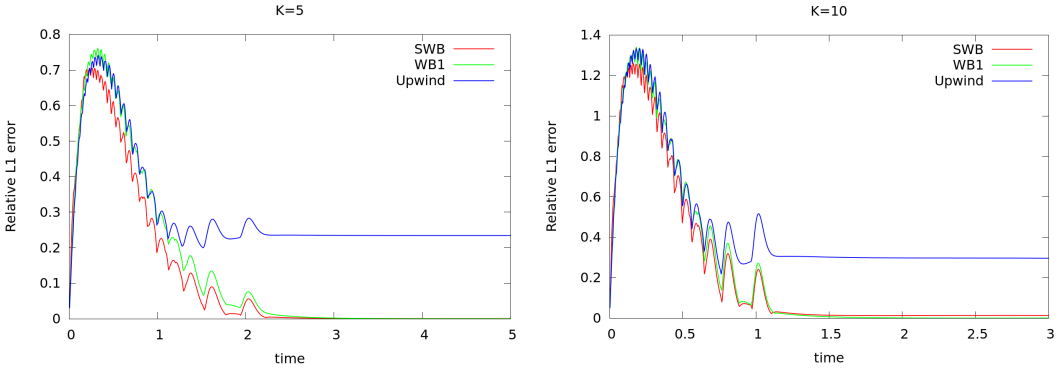

FIGURE 8: Relative L^1 error vs time, $T^f = 30$

In figure 9 are displayed the corresponding solutions at $T^f = 30$. In the picture the curves of the analytical solution and the numerical solutions of the SWB and WB1 schemes are merged, due to the fact that the error of the SWB and WB1 schemes are close to the computer zero. The peak of the analytical solution si not well retranscribed by the upwind scheme.

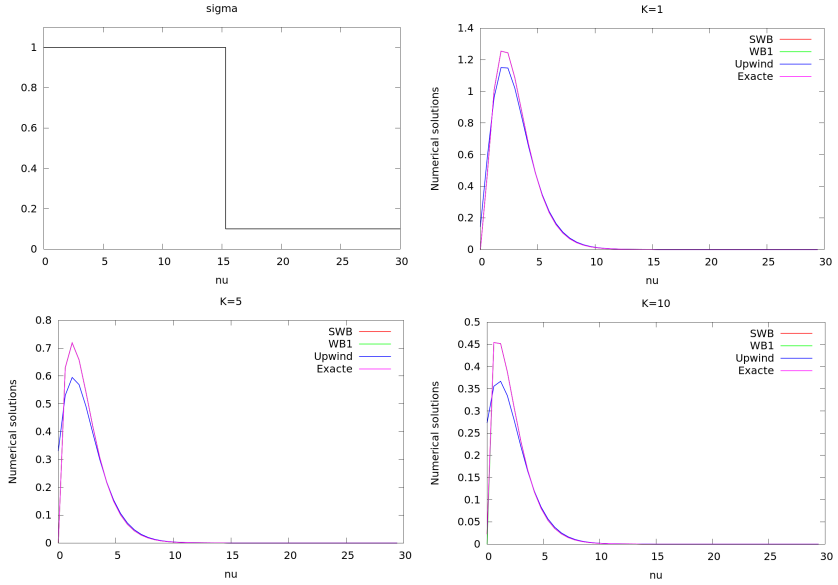

FIGURE 9: Corresponding solutions at t=30

For the second test case the emission absorption coefficient is still taken as a piecewise constant function but we took a negative κ. The initial condition are such that $\rho_j(0) = 0$. In figure 10 are displayed the evolution of the relative L^1 error as time goes on, for several value of κ. As previously, we see that the relative L^1 error of the upwind scheme increases with κ, and reaches roughly 20% for $\kappa = -10$.

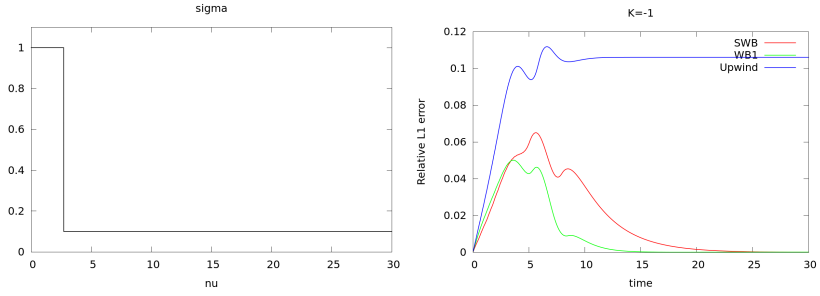

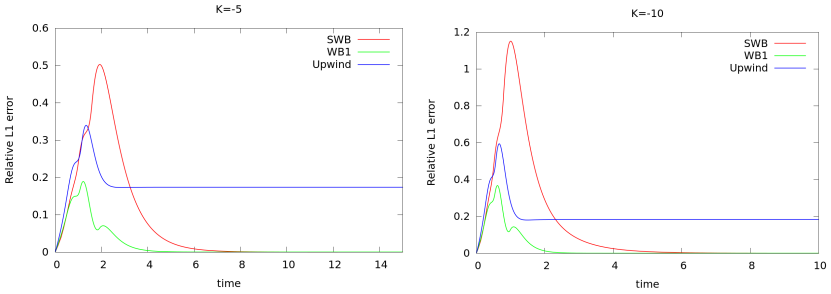

FIGURE 10: Relative L^1 error vs time, $T^f = 30$

The corresponding solutions at $T^f = 30$ are displayed in figure 11. Once again, the curves of the analytical solution and the numerical solutions of the SWB and WB1 schemes curves are merged, and the upwind scheme does not retranscribe faithfully the behavior of the analytical solution.

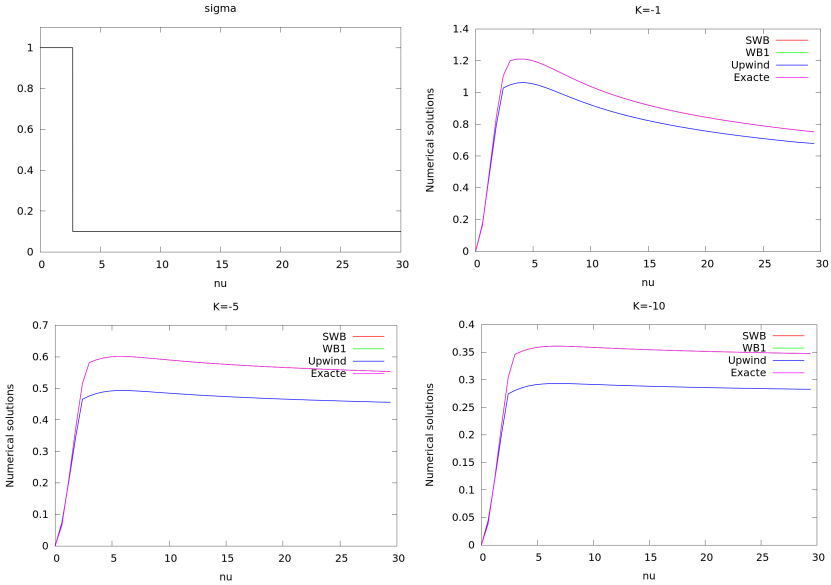

FIGURE 11: Corresponding solutions at t=30

4. CONCLUSION

The long time behavior of the Spectrally Well-Balanced scheme has been studied for several irregular opacities, including highly peaked emission absorption coefficient and the Cramer's opacity. In particular we proved that the well-balanced property of the scheme is preserved, and we studied numerically the consistency of the scheme as the velocity speed κ tends to 0 for these opacities. The case $\kappa < 0$ has also been studied, and the numerical results agree with the theoretical result (lemma 2.1). Finally, the advantage of the SWB scheme with respect to the upwind scheme has been shown in two test cases for different values of the coefficients κ and σ.

REFERENCES

[1] C. Buet, B. Depsrés *Asymptotic Analysis of Fluid Models for the Coupling of radiation and Hydrodynamics* JQSRT 85, pp 385-418, 2004.

[2] C. Bardos, F. Golse, B Perthame *The Rosseland Approximation for the Radiative Transfer Equations* Communications on Pure and Applied Mathematics, Vol XL, pp 691-721, 1987.

[3] C. Bardos, F. Golse, B. Perthame, R. Sentis *The Nonaccretive Radiative Transfer Equations: Existence of Solutions and Rosseland Approximation* Journal of Functional Analysis 77, pp 434-460, 1988.

[4] J. M. Greenberg, A. Y. Leroux *A Well-Balanced Scheme for the Numerical Processing of Source Terms in Hyperbolic Equations* Journal on Numerical Analysis 33 (1), pp 1-16 1996.

[5] P Godillon-Lafitte, T Goudon *A coupled model for radiative transfer: doppler effects, equilibrium, and nonequilibrium diffusion asymptotics* Multiscale Model. Simul. 4 (4), pp 1245-1279, 2005.

[6] L. Gosse, G. Toscani *An asymptotic preserving well-balanced scheme for the hyperbolic heat equations* C. R. Acad. Sci. Paris, Ser I 334, pp 337-342, 2002.

[7] T. Leroy, C. Buet, B. Després *A well-balanced scheme for a transport equation with varying velocity arising in relativistic transfer equation*, Springer Proceedings in Mathematics and Statistics 78, pp 891-899, 2014.

[8] T. Leroy *Relativistic transfer equations: maximum principle and convergence to the non-equilibrium regime*, HAL 2014, submitted to Kinetic and Related Models.